THE JOURNAL OF PHYSICAL CHEMISTRY B

Article

pubs.acs.org/JPCB

Notable Effects of Metal Salts on UV−Vis Absorption Spectra of α-, β-, γ-, and δ-Tocopheroxyl Radicals in Acetonitrile Solution. The Complex Formation between Tocopheroxyls and Metal Cations

Kazuo Mukai,* Yutaro Kohno, Aya Ouchi, and Shin-ichi Nagaoka

Department of Chemistry, Faculty of Science, Ehime University, Matsuyama 790-8577, Japan

Supporting Information

ABSTRACT: The measurements of the UV−vis absorption spectra of α-, β-, γ-, and δ-tocopheroxyl (α-, β-, γ-, and δ-Toc•) radicals were performed by reacting aroxyl (ArO•) radical with α-, β-, γ-, and δ-tocopherol (α-, β-, γ-, and δ-TocH), respectively, in acetonitrile solution including three kinds of alkali and alkaline earth metal salts ($LiClO_4$, $NaClO_4$, and $Mg(ClO_4)_2$) (MX or MX_2), using stopped-flow spectrophotometry. The maximum wavelengths (λ_{max}) of the absorption spectra of the α-, β-, γ-, and δ-Toc• located at 425−428 nm without metal salts increased with increasing concentrations of metal salts (0−0.500 M) in acetonitrile and approached some constant values, suggesting (Toc•···M^+ (or M^{2+})) complex formations. Similarly, the values of the apparent molar extinction coefficient (ε_{max}) increased drastically with increasing concentrations of metal salts in acetonitrile and approached some constant values. The result suggests that the formations of Toc• dimers were suppressed by the metal ion complex formations of Toc• radicals. The stability constants (K) were determined for Li^+, Na^+, and Mg^{2+} complexes of α-, β-, γ-, and δ-Toc•. The K values increased in the order of $NaClO_4$ < $LiClO_4$ < $Mg(ClO_4)_2$, being independent of the kinds of Toc• radicals. Furthermore, the K values increased in the order of δ- < γ- < β- < α-Toc• radicals for each metal salt. The alkali and alkaline earth metal salts having a smaller ionic radius of the cation and a larger charge of the cation gave a larger shift of the λ_{max} value, a larger ε_{max} value, and a larger K value. The result of the DFT molecular orbital calculations indicated that the α-, β-, γ-, and δ-Toc• radicals were stabilized by the (1:1) complex formation with metal cations (Li^+, Na^+, and Mg^{2+}). Stabilization energy (E_S) due to the complex formation increased in the order of Na^+ < Li^+ < Mg^{2+} complexes, being independent of the kinds of Toc• radicals. The calculated result also indicated that the metal cations coordinate to the O atom at the sixth position of α-, β-, γ-, and δ-Toc• radicals.

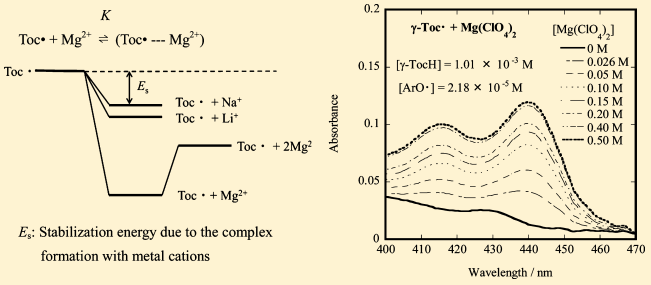

1. INTRODUCTION

It is well-known that lipophilic vitamin E (α-, β-, γ-, and δ-tocopherols, TocH) is localized in biomembranes and functions as an efficient inhibitor of lipid peroxidation.[1−3] The antioxidant actions of the TocH have been ascribed to the scavenging reaction of peroxyl (LOO•) radicals, producing the corresponding tocopheroxyl (Toc•) radicals (Figure 1) (reaction 1).[4] If the TocH exist in biomembranes and oils, the Toc• radicals may react with unsaturated lipids (LH) (reaction 2). Reaction 2 is known as a pro-oxidant reaction, which induces the degradation of unsaturated lipids.[5−10] Ubiquinol-10 ($UQ_{10}H_2$)[1,11−13] and/or vitamin C (ascorbate anion, AsH^-)[1,14−16] enhance the antioxidant activity of tocopherol by regenerating Toc• to tocopherol (reaction 3) to protect the above pro-oxidant effects. Further, Toc• radicals disappear by bimolecular reaction with another Toc• radical to give nonradical products (NRPs) (reaction 4).[4]

$$\mathrm{LOO^\bullet + TocH \xrightarrow{k_{inh}} LOOH + Toc^\bullet} \quad (1)$$

$$\mathrm{Toc^\bullet + LH \xrightarrow{k_p} TocH + L^\bullet} \quad (2)$$

$$\mathrm{Toc^\bullet + UQ_{10}H_2\ (and/or\ AsH^-) \xrightarrow{k_r} TocH + UQ_{10}H^\bullet\ (and/or\ As^{\bullet -})} \quad (3)$$

$$\mathrm{Toc^\bullet + Toc^\bullet \xrightarrow{2k_d} nonradical\ products\ (NRP)} \quad (4)$$

As described above, α-, β-, γ-, and δ- Toc• radicals are important key radicals, which appear in the process of the antioxidant and pro-oxidant actions of α-, β-, γ-, and δ-TocH. Detailed kinetic studies have been performed for the reactions 1,[2,4] 2,[10] 3,[11−16] and 4,[4,17−19] and the mechanisms involved have been studied extensively.

It is also well-known that relatively high concentrations of alkali and alkaline earth metal ions (Na^+, K^+, Mg^{2+}, and Ca^{2+}) are included in human blood, plasma, and various tissues.[20] These metal ions play important roles for many kinds of enzymatic reactions.[21] α-, β-, γ-, and δ-TocH coexist with these metal ions in the above biological systems.[22−24] However, the

Received: May 24, 2012
Revised: July 9, 2012
Published: July 9, 2012

 © 2012 American Chemical Society dx.doi.org/10.1021/jp305039z | J. Phys. Chem. B 2012, 116, 8930−8941

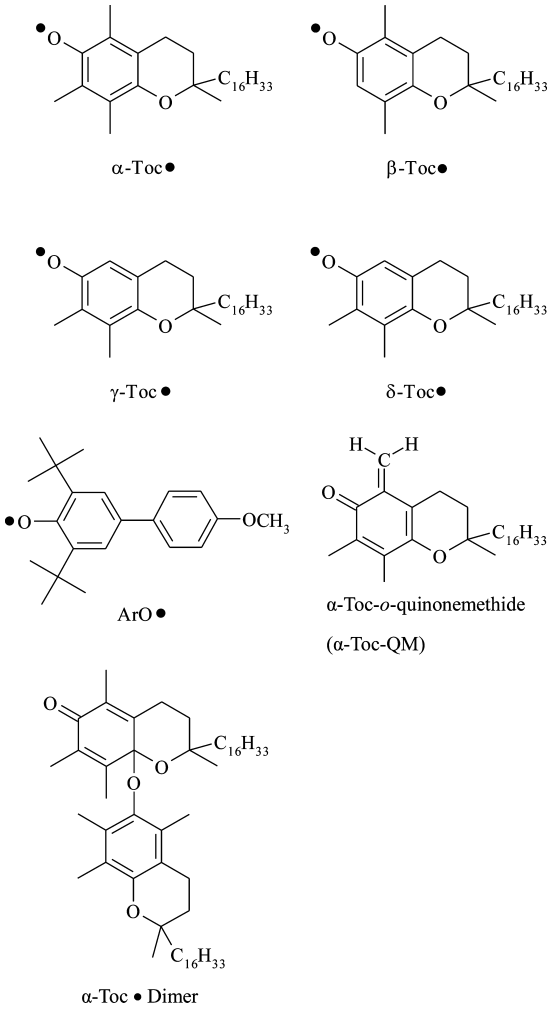

Figure 1. Molecular structures of α-, β-, γ-, and δ- tocopheroxyl (α-, β-, γ-, and δ-Toc$^{\bullet}$), aroxyl (ArO$^{\bullet}$) radical, α-Toc-*o*-quinonemethide (α-Toc-QM), and α-tocopheroxyl dimer (α-Toc$^{\bullet}$ Dimer).

examples of the kinetic studies of the effect of these metal ions on the free radical-scavenging reaction of the antioxidants including α-, β-, γ-, and δ-TocH are very limited.[25,26]

In previous works,[27,28] in order to clarify the effect of alkali and alkaline earth metal ions on the scavenging reaction of the free radical by α-TocH, we measured the second-order rate constants (k_s) for the reaction of α-TocH with 2,6-di-*t*-butyl-4-(4-methoxyphenyl)phenoxyl (aroxyl, ArO$^{\bullet}$) (see Figure 1) in protic methanol and aprotic acetonitrile solvents including various concentrations of metal salts (LiI, $LiClO_4$, NaI, $NaClO_4$, KI, and $Mg(ClO_4)_2$) (reaction 5), using stopped-flow spectrophotometry. The effects of these metal salts on the bimolecular self-reaction rate ($2k_d$) (reaction 4) and UV−vis absorption spectrum of α-Toc$^{\bullet}$ were also studied.

$$\text{ArO}^{\bullet} + \text{TocH} \xrightarrow{k_s} \text{ArOH} + \text{Toc}^{\bullet} \qquad (5)$$

Some notable effects of the metal salts were observed for (i) the rate constant (k_s), (ii) the rate constant ($2k_d$), and (iii) the maximum wavelength (λ_{max}) (and the molar extinction coefficient (ε_{max})) of α-Toc$^{\bullet}$ in acetonitrile.[28] Similarly, the effect of the metal salts was observed for the k_s value in methanol.[27] However, no effects of metal salts were observed for the $2k_d$ and λ_{max} (and ε_{max}) values in methanol. From the results, the mechanisms for reactions 4 and 5 were discussed.

Furthermore, recently, a kinetic study of the regeneration reaction of α-TocH by $UQ_{10}H_2$ (reaction 3) was performed in the presence of four kinds of alkali and alkaline earth metal salts ($LiClO_4$, $NaClO_4$, NaI, and $Mg(ClO_4)_2$) in methanol and acetonitrile solutions, using double-mixing stopped-flow spectrophotometry.[29] The second-order rate constants (k_r) for the reaction of α-Toc$^{\bullet}$ radical with $UQ_{10}H_2$ increased and decreased notably with increasing concentrations of metal salts in methanol and acetonitrile, respectively. The difference between the reaction mechanisms in methanol and acetonitrile solutions was discussed on the basis of the results obtained.

In the present work, the measurements of the UV−vis absorption spectra of α-, β-, γ-, and δ-Toc$^{\bullet}$ radicals were performed by reacting ArO$^{\bullet}$ radical with α-, β-, γ-, and δ-TocH, respectively, in acetonitrile solution including three kinds of alkali and alkaline earth metal salts ($LiClO_4$, $NaClO_4$, and $Mg(ClO_4)_2$), using stopped-flow spectrophotometry. Some notable effects of the metal salts were observed for the λ_{max} and ε_{max} values of α-, β-, γ-, and δ-Toc$^{\bullet}$ and the stability constants (K) for the complex formation between α-, β-, γ-, and δ-Toc$^{\bullet}$ and metal cations (Li^+, Na^+, and Mg^{2+}) in acetonitrile. Further, density functional theory (DFT) molecular orbital (MO) calculations were performed for the above metal complexes.

2. EXPERIMENTAL METHODS

2.1. Materials. The α-, β-, γ-, and δ-TocH was kindly supplied from Eisai Co. Ltd. $LiClO_4$, $NaClO_4$, and $Mg(ClO_4)_2$ are commercially available. Optical-grade acetonitrile was used for the measurement. Aroxyl (ArO$^{\bullet}$) radical was prepared according to the method of Rieker et al.[30]

2.2. Measurements. UV−vis absorption spectra of α-, β-, γ-, and δ-Toc$^{\bullet}$ radicals were obtained with a Unisoku Model RSP-1000 stopped-flow spectrophotometer by mixing equal volumes of acetonitrile solutions of α-, β-, γ-, and δ-TocH and ArO$^{\bullet}$ under nitrogen atmosphere, respectively.[28] The shortest time necessary for mixing two solutions and recording the first data point (that is, the dead time) was 10−20 ms. The reaction was monitored with either single-wavelength detection or a photodiode array detector attached to the stopped-flow spectrophotometer. All measurements were performed at 25.0 ± 0.5 °C.

2.3. Computational Method and Procedure. The experimental results on complex formation between Toc$^{\bullet}$ and metal cations were interpreted in light of DFT. These calculations were done at the B3LYP/6-31G**//B3LYP/6-31G** level using the Gaussian 09 program.[31] In the calculation of Toc$^{\bullet}$, its phytyl side chain was replaced by a methyl group (Figure 8). The geometries were optimized without imposing any structural constraint.

3. RESULTS

3.1. Effect of Metal Salts on UV−Vis Absorption Spectra of α-, β-, γ-, and δ-Toc$^{\bullet}$ Radicals in Acetonitrile Solution. The ArO$^{\bullet}$ radical is stable in the absence of β-, γ-, and δ-TocH and shows absorption peaks at λ_{max} = 374.4 (ε = 19100 M^{-1} cm^{-1}), and 577.9 nm (ε = 4200 M^{-1} cm^{-1}) in acetonitrile solution, as shown in Figure 2. By adding the acetonitrile solution of β- or γ-TocH to the solution of ArO$^{\bullet}$ (1:1 in volume) at 25.0 °C, the absorption of ArO$^{\bullet}$ disappeared quickly, and the spectrum was changed to that of β- or γ-Toc$^{\bullet}$ with weak absorption peaks at λ_{max} = 427.4 or 427.5 nm, respectively, as shown in Figure 2a,b (reaction 5). β- and γ-

dx.doi.org/10.1021/jp305039z | J. Phys. Chem. B 2012, 116, 8930−8941

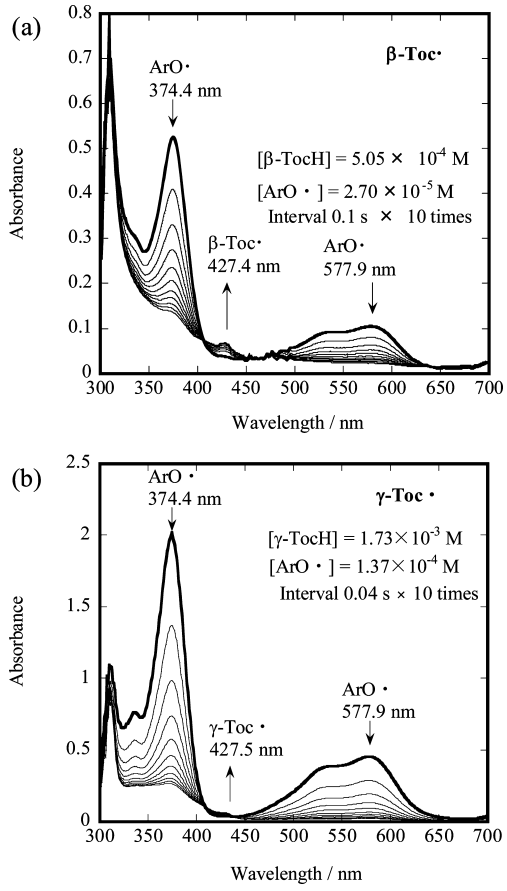

Figure 2. (a) Change in the electronic absorption spectrum of ArO• and β-Toc• radicals during the reaction of ArO• with β-TocH in acetonitrile solution at 25.0 °C. The spectra were recorded at 100 ms intervals. The arrow indicates a decrease (ArO•) and an increase (β-Toc•) in absorbance with time. $[ArO^{\bullet}]_{t=0}$ and $[\beta\text{-TocH}]_{t=0}$ indicate the concentrations obtained by mixing acetonitrile solutions of β-TocH (1.01×10^{-3} M) (cell A) and ArO• (5.40×10^{-5} M) (cell B) (1:1 in volume). (b) Change in the electronic absorption spectrum of ArO• and γ-Toc• radicals during the reaction of ArO• with γ-TocH in acetonitrile solution at 25.0 °C. The spectra were recorded at 40 ms intervals.

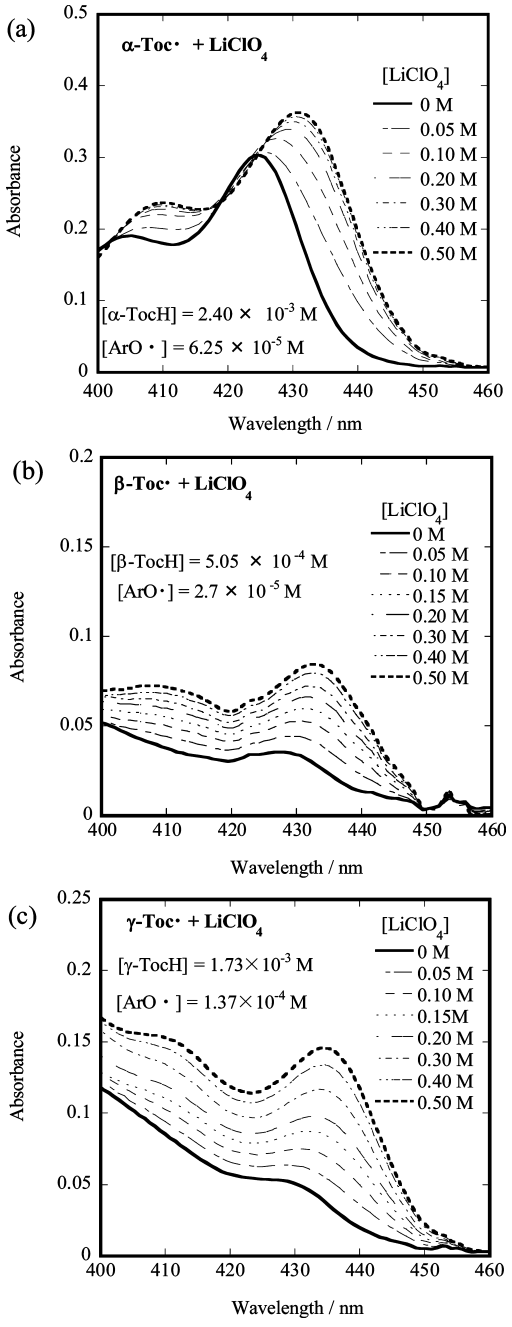

Figure 3. UV−visible absorption spectra at t_{max} for (a) α-Toc•, (b) β-Toc•, and (c) γ-Toc• radicals at 25.0 °C in acetonitrile solution including various concentrations of $LiClO_4$.

Toc• are unstable at 25.0 °C, and their absorption peaks decreased rapidly after passing through the maximum at t_{max}, as reported for the reaction in ethanol.[19] The spectra of the β- and γ-Toc• at t_{max} = ~400 and ~500 ms are shown in Figure 3b,c, respectively, together with that observed for α-Toc• radical (see Figure 3a).[28] δ-Toc• was unstable, and its absorption peak was not observed in the absence of metal salts.

Similar measurements were performed for β-, γ-, and δ-TocH in acetonitrile solution including various concentrations of the metal salts ($LiClO_4$, $NaClO_4$, and $Mg(ClO_4)_2$), where the same concentration of ArO• was used for each measurement. As shown in Figures 3−5, shifts of the absorption peaks (λ_{max}) of β- and γ-Toc• were observed in the presence of the $LiClO_4$, $NaClO_4$, and $Mg(ClO_4)_2$ salts, respectively. A weak absorption peak of δ-Toc• was observed only in the presence of $Mg(ClO_4)_2$ salt, as shown in Figure 5e.

The λ_{max} values of β- and γ-Toc• (427.4 and 427.5 nm) in the absence of metal salts increased with increasing concentrations of metal salts, respectively, and approached different constant values, depending on the kinds of metal salts, as shown in Figure 6b,c and as listed in Table 1. A large shift of the λ_{max} value of δ-Toc• was observed in the solution including $Mg(ClO_4)_2$ salt, as shown in Figure 6d and as listed in Table 1. As reported in a previous work,[28] similar results were obtained for α-Toc• radical in the presence of these metal salts (see Figures 3a−6a). In each Toc• radical, the λ_{max} value increased in the following order at the same concentration of the metal salts:

$$\lambda_{max}(\text{without metal salt}) < \lambda_{max}(NaClO_4) < \lambda_{max}(LiClO_4) < \lambda_{max}(Mg(ClO_4)_2) \quad (6)$$

dx.doi.org/10.1021/jp305039z | J. Phys. Chem. B 2012, 116, 8930−8941

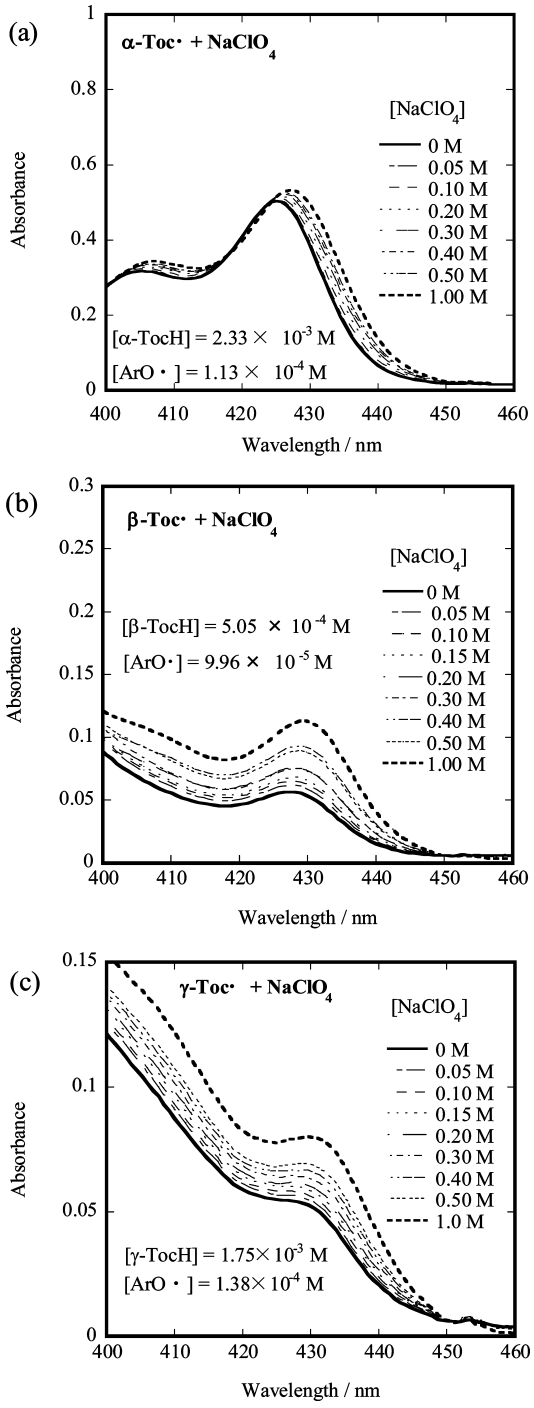

Figure 4. UV−visible absorption spectra at t_{max} for (a) α-Toc$^{\bullet}$, (b) β-Toc$^{\bullet}$, and (c) γ-Toc$^{\bullet}$ radical at 25.0 °C in acetonitrile solution including various concentrations of $NaClO_4$.

The result suggests the complex formation between α-, β-, γ-, and δ-Toc$^{\bullet}$ radicals and metal cations in acetonitrile. The stability constants (K) were determined for the metal cation complexes of α-, β-, γ-, and δ-Toc$^{\bullet}$ radicals by analyzing the change of the absorption spectra of the Toc$^{\bullet}$ radicals in the presence of metal salts, as described in the Discussion.

On the other hand, the shift of the absorption peak of ArO$^{\bullet}$ radical was not observed in the presence of all of the metal salts (0.500 M) used, as reported in a previous work.[28] The interactions between metal cations and ArO$^{\bullet}$ radical are considered to be negligible in acetonitrile.

3.2. Effect of Metal Salts on Molar Extinction Coefficients (ε) of α-, β-, γ-, and δ-Toc$^{\bullet}$ Radicals in Acetonitrile Solution. In addition to the shift of the absorption peak (λ_{max}), a remarkable increase of the absorbance (that is, an increase of the molar extinction coefficient (ε_{max})) of β-, γ-, and δ-Toc$^{\bullet}$ radicals was observed with increasing concentrations of metal salts, as shown in Figures 3−5. For example, the absorbance at t_{max} (A_{max}) of β-Toc$^{\bullet}$ radical increased from A_{max} = 0.0560 at $[Mg(ClO_4)_2]$ = 0 M to 0.276 at $[Mg(ClO_4)_2]$ = 0.50 M, when the same concentration of ArO$^{\bullet}$ was reacted with excess β-TocH, as shown in Figure 5c. Similarly, the absorbance of γ-Toc$^{\bullet}$ radical increased from A_{max} = 0.0257 at $[Mg(ClO_4)_2]$ = 0 M to 0.120 at $[Mg(ClO_4)_2]$ = 0.50 M, as shown in Figure 5d. Furthermore, the absorption of δ-Toc$^{\bullet}$ was observed in the presence of $Mg(ClO_4)_2$ salt, although it was negligible in the absence of $Mg(ClO_4)_2$ salt, as shown in Figure 5e. Such a remarkable increase of the absorption was not observed in the case of α-Toc$^{\bullet}$ (see Figure 5a).

The values of the apparent ε_{max} were tentatively estimated from A_{max} of the β-, γ-, and δ-Toc$^{\bullet}$ at t_{max} (see Figures 3−5) by assuming Lambert−Beer law ($A_{max} = \varepsilon_{max}[Toc^{\bullet}] = \varepsilon_{max}[ArO^{\bullet}]_{t=0}$), as performed for α-Toc$^{\bullet}$.[19,28] The values of ε_{max} obtained are listed in Table 2, and the plots of ε_{max} versus [metal salt] are shown in Figure 7. As observed for the λ_{max} values of β-, γ-, and δ-Toc$^{\bullet}$, the ε_{max} values also increased with increasing concentrations of metal salts and approached different constant values at high concentrations of metal salt, as shown in Figure 7 and as listed in Table 2. At the same concentration of metal salts, the ε_{max} value increased in the following order:

$$\varepsilon_{max}(\text{without metal salt}) < \varepsilon_{max}(NaClO_4) < \varepsilon_{max}(LiClO_4) < \varepsilon_{max}(Mg(ClO_4)_2) \quad (7)$$

The reason for such a remarkable increase of the ε_{max} values observed for β-, γ-, and δ-Toc$^{\bullet}$ will be discussed in the Discussion.

3.3. DFT Molecular Orbital Calculations for Metal Cation Complexes of α-, β-, γ-, and δ-Toc$^{\bullet}$ Model Radicals. As shown in Figure 6 and as listed in Table 1, shifts of the absorption peak (λ_{max}) of α-, β-, γ-, and δ-Toc$^{\bullet}$ were observed in the presence of the metal salts ($LiClO_4$, $NaClO_4$, and $Mg(ClO_4)_2$). The result suggests the complex formation between α-, β-, γ-, and δ-Toc$^{\bullet}$ and metal cations (Li^+, Na^+, and Mg^{2+}) in acetonitrile solution. Accordingly, some calculations based on DFT[31] at the level of B3LYP/6-31G**//B3LYP/6-31G** were performed for (i) metal cation-free α-, β-, γ-, and δ-Toc$^{\bullet}$ models (α-, β-, γ-, and δ-Toc$^{\bullet}$−M) and (ii) their complexes with metal cations (Li^+, Na^+, and Mg^{2+}) in the vapor phase. In Toc$^{\bullet}$−M, the phytyl side chain of Toc$^{\bullet}$ is replaced by a methyl group (Figure 8).

Mulliken atomic charges (Z) were calculated for geometry-optimized metal cation-free α-, β-, γ-, and δ-Toc$^{\bullet}$−M radicals. The result indicates that O-1 and O-6 atoms in α-, β-, γ-, and δ-Toc$^{\bullet}$−M (Figure 8) have large negative charges, as listed in Table 3. The Z values on the O-6 atom (and O-1 atom) of the α-, β-, γ-, and δ-Toc$^{\bullet}$−M are similar to each other. Further, the absolute values of negative charge on O-1 and O-6 atoms are

dx.doi.org/10.1021/jp305039z | J. Phys. Chem. B 2012, 116, 8930−8941

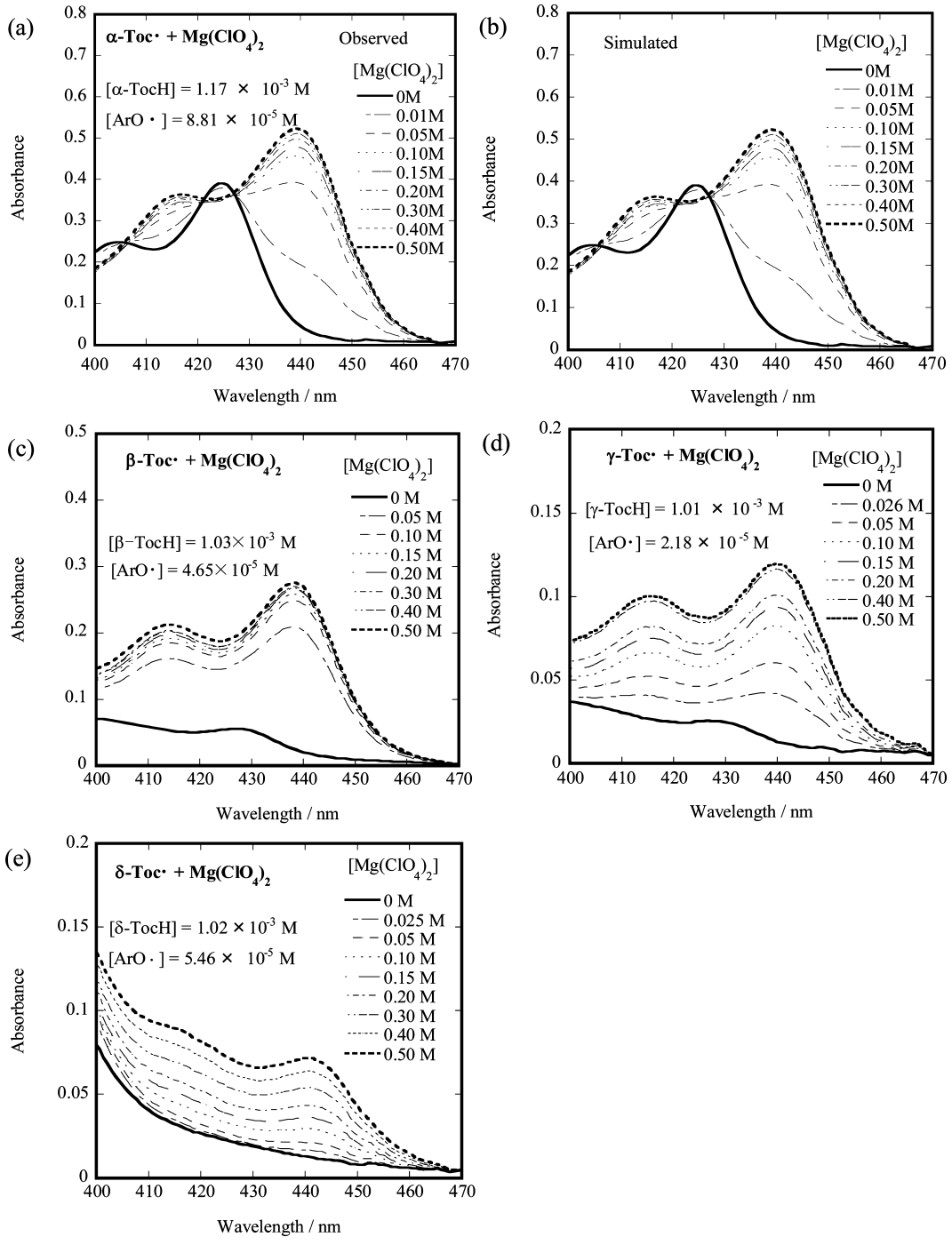

Figure 5. UV−visible absorption spectra at t_{max} for (a) α-Toc$^{\bullet}$ (observed), (b) α-Toc$^{\bullet}$ (simulated), (c) β-Toc$^{\bullet}$, (d) γ-Toc$^{\bullet}$, and (e) δ-Toc$^{\bullet}$ radicals at 25.0 °C in acetonitrile solution including various concentrations of $Mg(ClO_4)_2$).

larger than those on the other carbon atoms with negative charge (see the Supporting Information).

Consequently, as the positions of the metal cations in the complex, the following two cases 1 and 2 were assumed, where metal cations coordinate to O-6 and O-1 atoms, respectively, in α-, β-, γ-, and δ-Toc$^{\bullet}$−M. The structures in the cases for the Mg^{2+} complex of α-Toc$^{\bullet}$−M radical are shown in Figure 8. The metal cations may also interact with the π-electrons delocalized on the aromatic ring of α-Toc$^{\bullet}$−M (case 3). Furthermore, two metal cations coordinate to O-6 and O-1 atoms at the same time and may form the (1:2) complex with α-Toc$^{\bullet}$−M, as shown in case 4. Geometry optimization of the metal complexes in the four cases was performed, and the stabilization energy (E_S) of α-Toc$^{\bullet}$−M due to the complex formation between α-Toc$^{\bullet}$−M and the Mg^{2+} ion was calculated for these cases 1−4. As listed in Table 4, the E_S values increased in the following order:

$$E_S(\text{case 4}) < E_S(\text{case 3}) < E_S(\text{case 2}) < E_S(\text{case 1}) \quad (8)$$

In cases 1−3, total energies of metal cation-free α-Toc$^{\bullet}$−M radical were stabilized by 799.7, 657.4, and 626.8 kJ/mol, respectively, owing to the (1:1) complex formation between α-Toc$^{\bullet}$−M and the Mg^{2+} ion. The largest stabilization energy (E_S) was obtained in the coordination of the Mg^{2+} ion to the O-

dx.doi.org/10.1021/jp305039z | J. Phys. Chem. B 2012, 116, 8930−8941

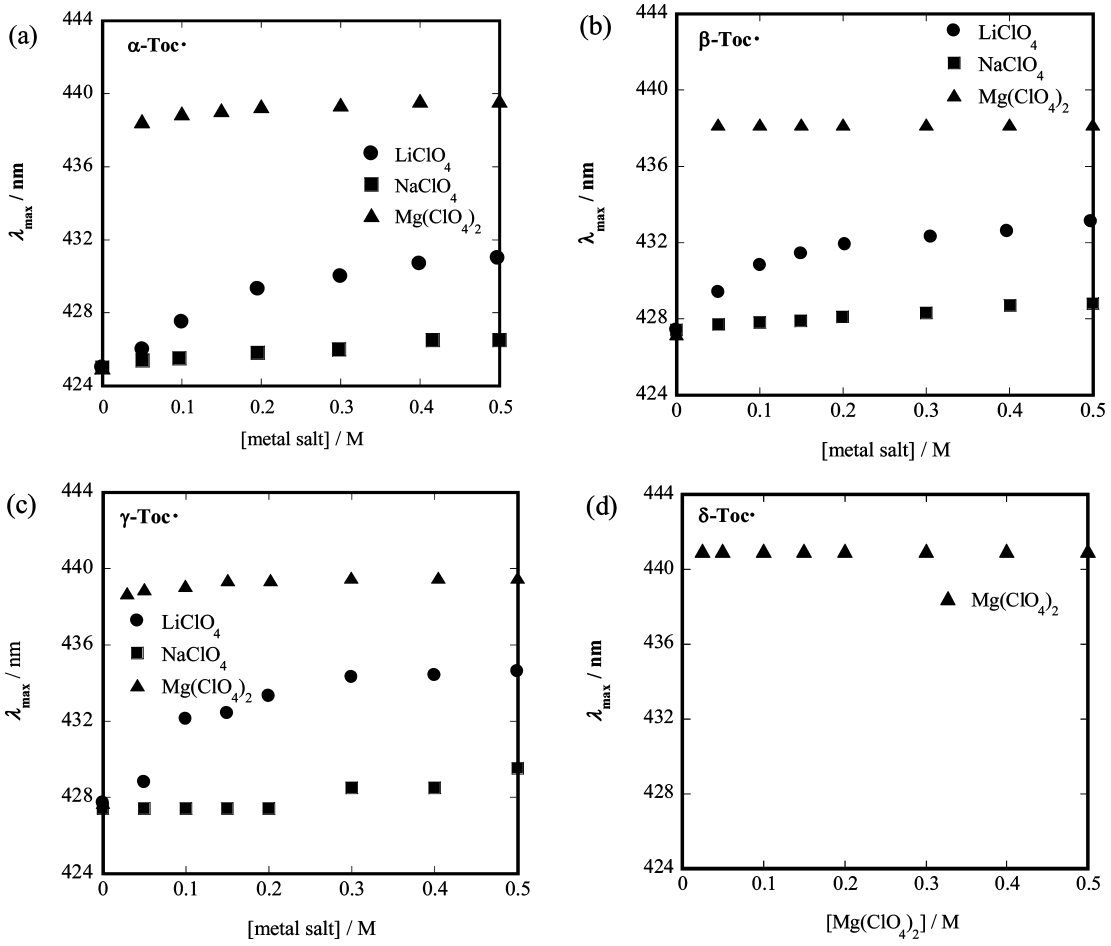

Figure 6. Plots of the peak wavelength (λ_{max}) of (a) α-Toc$^{\bullet}$, (b) β-Toc$^{\bullet}$, (c) γ-Toc$^{\bullet}$, and (d) δ-Toc$^{\bullet}$ radicals versus the concentration of metal salts ((●) $LiClO_4$, (■) $NaClO_4$, and (▲) $Mg(ClO_4)_2$).

Table 1. Values of UV−Visible Peak Wavelengths (λ_{max}) of the α-, β-, γ-, and δ-Toc$^{\bullet}$ Radicals in Acetonitrile Solution Including 0.00 and 0.50 M Metal Salts ($LiClO_4$, $NaClO_4$, and $Mg(ClO_4)_2$) at 25.0 °C, and Shifts in Wavelength (λ_{max}(0.50 M) − λ_{max}(0.00 M))

		$\lambda_{max}{}^{a}$/nm		
	[salt]/M	$LiClO_4$	$NaClO_4$	$Mg(ClO_4)_2$
α-Toc$^{\bullet}$	0.00	425.0	425.0	425.0
	0.50	431.0	426.5	439.2
	λ_{max}(0.50 M) − λ_{max}(0.00 M)	6.0	2.0	14.6
β-Toc$^{\bullet}$	0.00	427.4	427.4	426.5
	0.50	433.1	428.8	438.2
	λ_{max}(0.50 M) − λ_{max}(0.00 M)	5.7	1.8	11.7
γ-Toc$^{\bullet}$	0.00	427.5	427.5	427.5
	0.50	434.6	429.5	439.5
	λ_{max}(0.50 M) − λ_{max}(0.00 M)	7.1	2.0	12.0
δ-Toc$^{\bullet}$	0.00			
	0.50			441.0
	λ_{max}(0.50 M) − λ_{max}(0.00 M)			

[a]Experimental errors in the λ_{max} values observed for α-, β-, and γ-Toc$^{\bullet}$ with and without metal salts are ±0.5 nm.

Table 2. Values of Molar Extinction Coefficients (ε_{max}) of the α-, β-, γ-, and δ-Toc$^{\bullet}$ Radicals in Acetonitrile Solution Including 0.00 and 0.50 M Metal Salts ($LiClO_4$, $NaClO_4$, and $Mg(ClO_4)_2$) at 25.0 °C and the Ratio of Molar Extinction Coefficients (ε_{max}(0.50 M)/ε_{max}(0.00 M))

		$\varepsilon_{max}{}^{a}$/M^{-1}cm^{-1}		
	[salt]/M	$LiClO_4$	$NaClO_4$	$Mg(ClO_4)_2$
α-Toc$^{\bullet}$	0.00	4320	4320	4320
	0.50	5250	4480	5830
	ε_{max}(0.50 M)/ε_{max}(0.00 M)	1.22	1.04	1.35
β-Toc$^{\bullet}$	0.00	1170	1250	1140
	0.50	2980	2060	5870
	ε_{max}(0.50 M)/ε_{max}(0.00 M)	2.55	1.64	5.14
γ-Toc$^{\bullet}$	0.00	365	347	400
	0.50	1040	455	4170
	ε_{max}(0.50 M)/ε_{max}(0.00 M)	2.85	1.31	10.4
δ-Toc$^{\bullet}$	0.00	∼100[b]	∼100[b]	∼100[b]
	0.50			1210
	ε_{max}(0.50 M)/ε_{max}(0.00 M)			12.1

[a]Experimental errors in the ε_{max} values observed for α-, β-, and γ-Toc$^{\bullet}$ with and without metal salts are ±7%. [b]The ε_{max} value determined from an intercept at the vertical axis of the ε_{max} vesus $[Mg(ClO_4)_2]$ plot in Figure 7d.

6 atom (case 1). As listed in Table 4, the energy of metal cation-free α-Toc$^{\bullet}$−M was stabilized 400.9 kJ/mol by the (1:2) complex formation between α-Toc$^{\bullet}$−M and two Mg^{2+} ions (case 4). The energy of the (1:1) complex in case 1 was remarkably unstabilized by the coordination of another Mg^{2+} ion to the O-1 atom. The result suggests that the Mg^{2+} ion

dx.doi.org/10.1021/jp305039z | J. Phys. Chem. B 2012, 116, 8930−8941

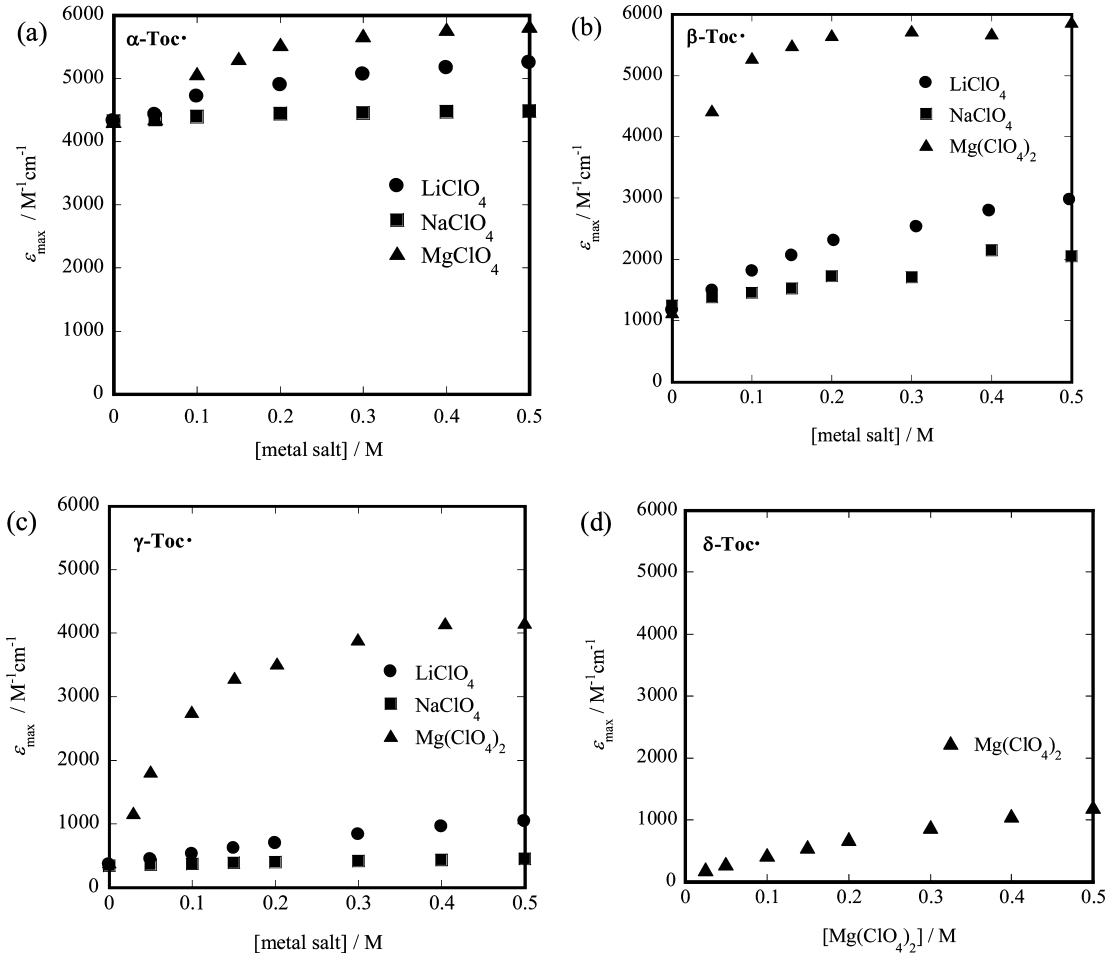

Figure 7. Plots of the molar extinction coefficient (ε_{max}) of (a) α-Toc$^{\bullet}$, (b) β-Toc$^{\bullet}$, (c) γ-Toc$^{\bullet}$, and (d) δ-Toc$^{\bullet}$ radicals versus the concentration of metal salts ((●) $LiClO_4$, (■) $NaClO_4$, and (▲) $Mg(ClO_4)_2$).

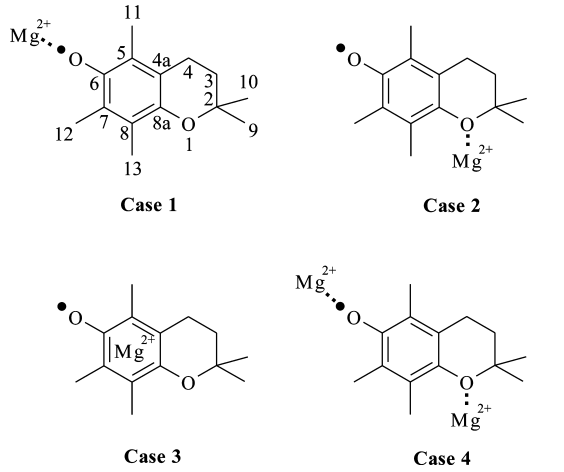

Figure 8. Four kinds of structures (cases 1–4) assumed for the complexes between the α-Toc$^{\bullet}$ model radical and the Mg^{2+} ion.

occupies a position near the O-6 atom in the Mg^{2+} complex (case 1) and forms only a stable (1:1) complex with α-Toc$^{\bullet}$–M in acetonitrile solution.

Similar calculations were performed for the Li^+ and Na^+ complexes of α-Toc$^{\bullet}$–M. The E_S values increased almost in the order of eq 8, as obtained for the Mg^{2+} complex (see Table 4).

Table 3. Mulliken Atomic Charges (*Z*) on O-1 and O-6 Atoms in α-, β-, γ-, and δ-Toc$^{\bullet}$ Model Radicals without the Phytyl Side Chain

	Z on O-1 atom	Z on O-6 atom
α-Toc$^{\bullet}$	−0.5431	−0.5228
β-Toc$^{\bullet}$	−0.5401	−0.5191
γ-Toc$^{\bullet}$	−0.5402	−0.5182
δ-Toc$^{\bullet}$	−0.5370	−0.5143

The result indicates that both the Li^+ and Na^+ ions also form only a (1:1) complex of case 1 with α-Toc$^{\bullet}$–M.

Furthermore, in all cases, the E_S values for the complex formation of α-Toc$^{\bullet}$–M increased in the following order (see Figure 9):

$$E_S(Na^+) < E_S(Li^+) < E_S(Mg^{2+}) \quad (9)$$

The stabilization energy (E_S) of β-, γ-, and δ-Toc$^{\bullet}$–M for the cases 1 and 2 also increased in the order of eq 9. The E_S values for the Mg^{2+} complex of α-, β-, γ-, and δ-Toc$^{\bullet}$–M in case 1 are very large (799.7–786.8 kJ/mol) and similar to each other. The E_S values for the Mg^{2+} complex are about 2.79–2.66 and 3.83–3.59 times as large as those for Li^+ (286.7–295.8 kJ/mol) and Na^+ (208.6–219.0 kJ/mol) complexes, respectively.

As listed in Table 5, the distances (r) between the metal cation and O-6 atom obtained for optimized α-, β-, γ-, and δ-Toc$^{\bullet}$–M complexes (case 1) are similar to one another in each

dx.doi.org/10.1021/jp305039z | J. Phys. Chem. B 2012, 116, 8930–8941

Table 4. Stabilization Energy (E_S) for the Complex Formation Between α-, β-, γ-, and δ-Toc$^\bullet$ Model Radicals and Metal Cations (Li^+, Na^+, and Mg^{2+})

		E_S/kJ·mol^{-1}			
		α-Toc$^\bullet$−M	β-Toc$^\bullet$−M	γ-Toc$^\bullet$−M	δ-Toc$^\bullet$−M
case 1	Li^+	286.7	291.8	291.0	295.8
	Na^+	208.6	214.9	214.0	219.0
	Mg^{2+}	799.7	793.7	792.5	786.8
case 2	Li^+	183.1	175.9	176.4	169.0
	Na^+	115.5	109.4	103.1	103.3
	Mg^{2+}	657.4	630.3	628.3	
case 3	Li^+	174.9		170.0	
	Na^+				
	Mg^{2+}	626.8			
case 4	Li^+	220.8			
	Na^+	109.1			
	Mg^{2+}	400.9		387.0	

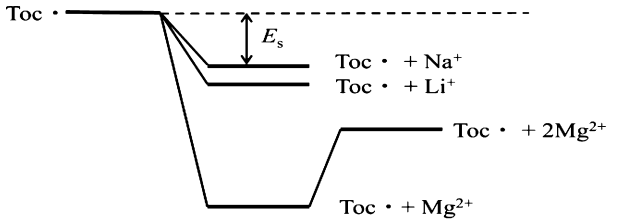

Figure 9. Changes of the energy levels of α-, β-, γ-, and δ-Toc$^\bullet$ radicals induced by the complex formation with metal cations (Li^+, Na^+, and Mg^{2+}). The figure shows that the energy level of the Toc$^\bullet$ radical is lowered by the (1:1) complex formation between Toc$^\bullet$ and metal cations.

of the Li^+, Na^+, and Mg^{2+} ions. The ionic radius of Li^+ (0.76 Å) is by 0.26 Å smaller than that of Na^+ (1.02 Å) (see Table 6). In fact, the distances (r(Li^+−O-6)) (1.698−1.703 Å) between the Li^+ ion and O-6 atom calculated for α-, β-, γ-, and δ-Toc$^\bullet$−M are by ∼0.35 Å smaller than those (r(Na^+−O-6)) (2.054−2.061 Å) between the Na^+ ion and O-6 atom. Consequently, a larger E_S was obtained for the Li^+ ion complex because the Coulomb interaction energy for Li^+ is larger than that for Na^+.

The ionic radius of Mg^{2+} (0.72 Å) is by 0.04 Å smaller than (or similar to) that of Li^+ (0.76 Å). However, the distances (r(Mg^{2+}−O-6)) (1.886−1.926 Å) between the Mg^{2+} ion and O-6 atom calculated for α-, β-, γ-, and δ-Toc$^\bullet$−M are by ∼0.20 Å larger than those (r(Li^+−O-6)) (1.698−1.703 Å) between the Li^+ ion and O-6 atom. On the other hand, the E_S value increases in the order of eq 9, as described above. As the Mg^{2+} ion has a larger positive charge than the Li^+ ion, the former will show stronger Coulomb interaction with the O-6 atom in α-, β-, γ-, and δ-Toc$^\bullet$−M than the latter, showing a larger E_S.

As described above, the negative charges (Z = −0.5370 to −0.5431) on the O-1 atom of α-, β-, γ-, and δ-Toc$^\bullet$−M are similar to each other and are by about 0.02−0.03 more negative than those (Z = −0.5143 to −0.5228) on the O-6 atom (see Table 3). As the charge on the O-1 atom is more negative than that on the O-6 atom, the former would show stronger Coulomb interaction with metal cations than the latter if the distances between metal cations and the O-1 and O-6 atoms were similar to each other. However, for instance, in α-Toc$^\bullet$−M, the distances (r(M^+ (or M^{2+})−O-1)) for Li^+, Na^+, and Mg^{2+} in case 2 are by 0.129, 0.153, and 0.394 Å larger than the corresponding ones (r(M^+ (or M^{2+})−O-6)) in case 1, respectively (see Table 5). This may be the reason why the stabilization energy increases in the order of eq 8.

Table 6. Values of Stability Constants (K) of the Li^+, Na^+, and Mg^{2+} Complexes with α-, β-, γ-, and δ-Toc$^\bullet$ Radicals in Acetonitrile at 25.0 °C and Ionic Radii of the Cations

	K^a/M^{-1}		
	$LiClO_4$	$NaClO_4$	$Mg(ClO_4)_2$
α-Toc$^\bullet$	9.2	2.8	45
β-Toc$^\bullet$	2.4	0.85	36
γ-Toc$^\bullet$	1.1	0.44	11
δ-Toc$^\bullet$			0.97
ionic radius/Å	0.76	1.02	0.72

[a]Experimental errors are ±10%.

4. DISCUSSION

4.1. Complex Formation between α-, β-, γ-, and δ-Toc$^\bullet$ Radicals and Metal Cations in Acetonitrile Solution. As shown in Figures 3−6 and as listed in Table 1, the λ_{max} values of α-, β-, γ-, and δ-Toc$^\bullet$ without metal salts increase with increasing concentrations of the metal salts in acetonitrile, suggesting the (Toc$^\bullet$···M^+ (or M^{2+})) complex formation between Toc$^\bullet$ radicals and metal cations. If the M^+ ion forms a (1:1) complex with Toc$^\bullet$, the following equilibrium between Toc$^\bullet$ and the M^+ ion may exist in acetonitrile solution.

$$\text{Toc}^\bullet + M^+ \overset{K}{\rightleftharpoons} (\text{Toc}^\bullet \cdots M^+) \quad (10)$$

$$K = \frac{[\text{Toc}^\bullet \cdots M^+]}{[\text{Toc}^\bullet][M^+]} \quad (11)$$

where K is a stability constant for eq 10. With increasing concentrations of the metal salts, the concentrations of the complex ([Toc$^\bullet$···M^+]) will increase rapidly; thus, the shifts of the absorption maximum (λ_{max}) proceed.

Table 5. Optimized Distances (r/Å) between Metal Cations (Li^+, Na^+, and Mg^{2+}) and O-6 (and O-1) Atoms in α-, β-, γ-, and δ-Toc$^\bullet$ Model Radical Complexes

	case 1			case 2			case 4		
	Li^+	Na^+	Mg^{2+}	Li^+	Na^+	Mg^{2+}	Li^+	Na^+	Mg^{2+}
α-Toc$^\bullet$	1.698	2.058	1.926	1.827	2.211	2.320	(O-6) 1.755 (O-1) 1.876	(O-6) 2.216 (O-1) 2.296	(O-6) 1.833 (O-1) 1.954
β-Toc$^\bullet$	1.703	2.061	1.911	1.831	2.215	2.299			
γ-Toc$^\bullet$	1.702	2.059	1.905	1.830	2.225	2.339	(O-6) 1.838 (O-1) 1.955		
δ-Toc$^\bullet$	1.701	2.054	1.886	1.834	2.223				

dx.doi.org/10.1021/jp305039z | J. Phys. Chem. B 2012, 116, 8930−8941

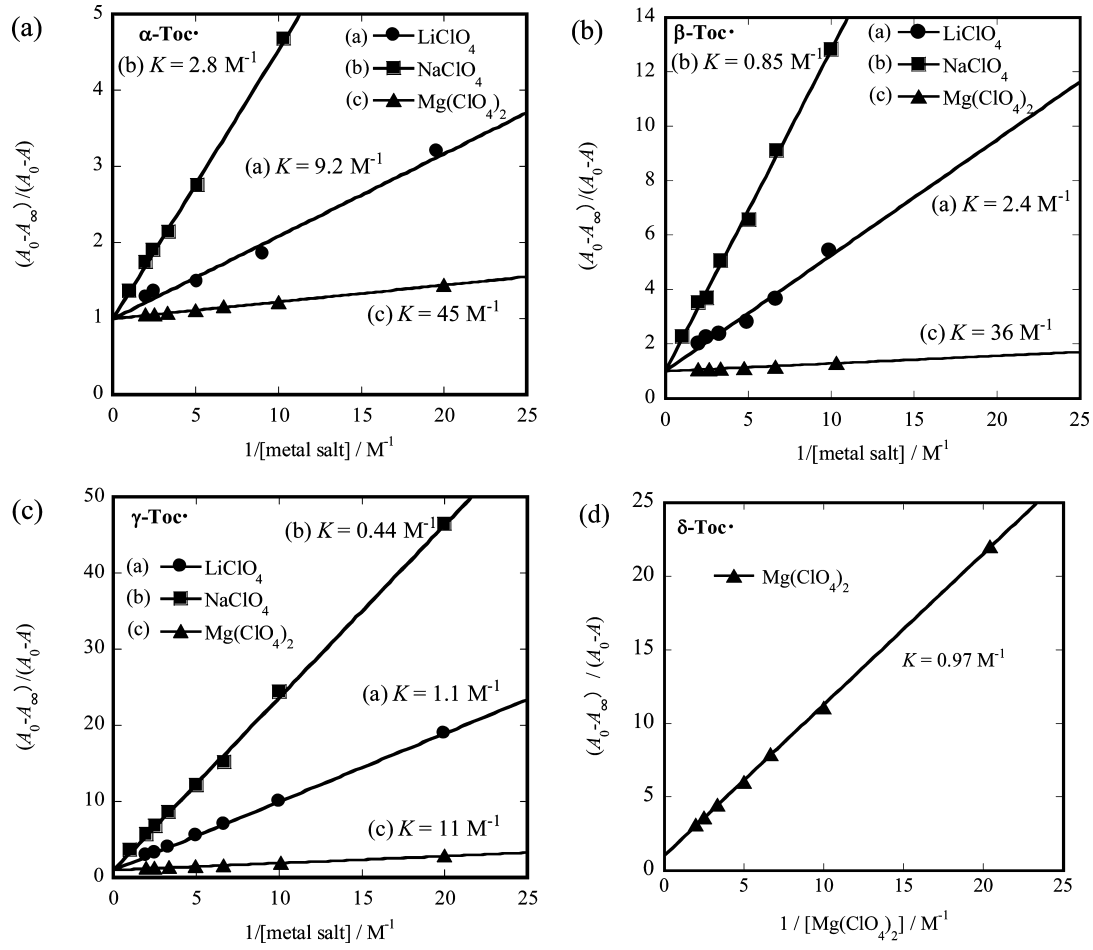

Figure 10. Plots of $(A_0 - A_\infty)/(A_0 - A)$ versus the inverse concentration of metal salts ($[\text{metal salt}]^{-1}$) ((●) $LiClO_4$, (■) $NaClO_4$, and (▲) $Mg(ClO_4)_2$). (a) α-Toc•, (b) β-Toc•, (c) γ-Toc•, and (d) δ-Toc•. Measurements were performed in acetonitrile at 25.0 °C.

The stability constant (K) may be determined using the following equation.[32]

$$\frac{(A_0 - A_\infty)}{(A_0 - A)} = 1 + \frac{1}{K[M^+]} \quad (12)$$

where A is the absorbance at a fixed wavelength of interest in the 425−445 nm region in the presence of a certain concentration of M^+ ion. A_0 and A_∞ are the absorbances at the same wavelength in the absence of the M^+ ion and in the presence of a large excess of the M^+ ion, sufficient to form the complex up to >99%, respectively. $(A_0 - A_\infty)/(A_0 - A)$ versus $[M^+]^{-1}$ plots for α-, β-, γ-, and δ-Toc• are shown in Figure 10a−d, respectively, indicating the formation of (1:1) complexes. The stability constants (K) obtained from the slopes in Figure 10b−d are listed in Table 6, together with those reported for α-Toc• (Figure 10a). The values of K for α-, β-, γ-, and δ-Toc• increase in the following order for any Toc• radical:

$$K(NaClO_4) < K(LiClO_4) < K(Mg(ClO_4)_2) \quad (13)$$

Furthermore, the values of K in acetonitrile solution including the metal salts ($LiClO_4$, $NaClO_4$, and $Mg(ClO_4)_2$) increase in the following order, being independent of the kinds of metal salts.

$$K(\delta\text{-Toc}^\bullet) < K(\gamma\text{-Toc}^\bullet) < K(\beta\text{-Toc}^\bullet) < K(\alpha\text{-Toc}^\bullet) \quad (14)$$

As reported in a previous work,[27] the effect of the metal salts (LiI, $LiClO_4$, NaI, $NaClO_4$, KI, and $Mg(ClO_4)_2$) on the UV−vis absorption spectrum of α-Toc• radical was negligible in protic methanol solvent, suggesting that the complex formations between the α-Toc• radical molecule and metal cations are hindered by the hydrogen bonds between α-Toc• radical and methanol molecules. On the other hand, notable effects of the metal salts ($LiClO_4$, $NaClO_4$, and $Mg(ClO_4)_2$) on the spectrum of α-Toc• were observed in aprotic acetonitrile solvent.[28] Similarly, in the present study, notable effects of the metal salts on the UV−vis absorption spectra of β-, γ-, and δ-Toc• were observed in acetonitrile solvent.

In fact, the results of DFT calculation indicated that the metal cations (Li^+, Na^+, and Mg^{2+}) form a stable (1:1) complex with α-, β-, γ-, and δ-Toc• model radicals (see Table 4). The formation of a (Toc•···M^+ (or M^{2+})) complex will be due to the Coulomb interaction between the metal cation (M^+ or M^{2+}) and the O-6 atom having large negative charge in Toc• radical molecules.

The distances (r) between the metal cations and O-6 atom in geometry-optimized α-, β-, γ-, and δ-Toc• model radicals were 1.698−1.703 Å for Li^+, 2.054−2.061 Å for Na^+, and 1.886−1.926 Å for Mg^{2+}, as listed in Table 5. The complex of $LiClO_4$ has a shorter distance r and shows a larger λ_{max} shift and a larger K value than the complex of $NaClO_4$. On the other hand, although the distances r for Mg^{2+} (1.886−1.926 Å) are larger than those for Li^+ (1.698−1.703 Å), the shifts of the λ_{max} value

dx.doi.org/10.1021/jp305039z | J. Phys. Chem. B 2012, 116, 8930−8941

for $Mg(ClO_4)_2$ are larger than those for $LiClO_4$. The result indicates that the Mg^{2+} ion having a larger positive charge of +2e gives a larger shift of the λ_{max} value and a larger K value because of the larger Coulomb interaction in $Mg(ClO_4)_2$ than that in $LiClO_4$.

Fukuzumi and Ohkubo[33] reported that the g_{zz} value of the ESR spectrum of the superoxide anion ($O_2^{\bullet-}$) radical decreases remarkably by the complex formation with metal ions (Li^+, Na^+, and Mg^{2+}) and that the decrease of the g_{zz} value depends on the Lewis acidity of metal ions.

4.2. α-Toc• Radical Forming a (1:1) Complex with Metal Cations in Acetonitrile Solution. As described above, the values of the stability constant (K) were determined for Toc•−Metal complexes by assuming a (1:1) complex formation between Toc• and the M^+ (or M^{2+}) ion. As shown in Figure 5a, a remarkable change of the UV−vis absorption spectrum of α-Toc• was observed with increasing concentrations of $Mg(ClO_4)_2$ salt, showing three isosbestic points at 406, 422, and 427 nm. α-Toc• radical shows two absorption peaks at 405.2 and 425.0 nm in the 400−470 nm region in the absence of $Mg(ClO_4)_2$ salt and at 417.1 and 439.2 nm in the presence of a high concentration (0.50 M) of $Mg(ClO_4)_2$ salt. On the other hand, a complex absorption spectrum was observed for the solution including a low concentration (0.010 M) of $Mg(ClO_4)_2$ salt.

If only the Mg^{2+}-free α-Toc• radical and a certain (1:1) complex coexist in acetonitrile solution (see eq 10), the absorption spectrum of α-Toc• (Abs_{obsd}) including a certain concentration of $Mg(ClO_4)_2$ salt will be explained by the sum of those for the Mg^{2+}-free α-Toc• radical (Abs_{free}) and the (1:1) complex ($Abs_{complex}$).

$$Abs_{obsd} = f_{free}Abs_{free} + f_{complex}Abs_{complex} \quad (15)$$

where f_{free} and $f_{complex}$ are mole fractions of Mg^{2+}-free α-Toc• and the (1:1) complex (α-Toc•···Mg^{2+}), respectively. f_{free} and $f_{complex}$ will be expressed as eqs 16 and 17, respectively. Here, as $Abs_{complex}$ (that is, the spectrum for the (1:1) complex), the spectrum observed for $[Mg(ClO_4)_2]$ = 0.500 M was used for the calculation.

$$f_{free} = \frac{[\alpha\text{-Toc}^\bullet]}{[\alpha\text{-Toc}^\bullet] + [\alpha\text{-Toc}^\bullet\cdots Mg^{2+}]} \quad (16)$$

$$f_{complex} = \frac{[\alpha\text{-Toc}^\bullet\cdots Mg^{2+}]}{[\alpha\text{-Toc}^\bullet] + [\alpha\text{-Toc}^\bullet\cdots Mg^{2+}]} \quad (17)$$

where [α-Toc•] and [α-Toc•···Mg^{2+}] are concentrations of Mg^{2+}-free α-Toc• and the (1:1) complex, respectively, in acetonitrile solution including a certain concentration of $Mg(ClO_4)_2$ salt. $[ArO^\bullet]_{t=0}$ is the initial concentration of ArO• radical used for reaction 5 and equals the sum of [α-Toc•] and [α-Toc•···Mg^{2+}].

$$[\alpha\text{-Toc}^\bullet] + [\alpha\text{-Toc}^\bullet\cdots Mg^{2+}] = [ArO^\bullet]_{t=0} \quad (18)$$

Using the value of K observed and eq 18, we can determine the concentrations, [α-Toc•] and [α-Toc•···Mg^{2+}], that is, the values of f_{free} and $f_{complex}$ in acetonitrile solution. Plots of mole fractions (f_{free} and $f_{complex}$) versus concentrations of $Mg(ClO_4)_2$ are shown in Figure 11.

Consequently, the simulation of the absorption spectra (Abs_{obsd}) of α-Toc• radical in acetonitrile solution including $Mg(ClO_4)_2$ salt was performed using eq 15. As shown in Figure 5a,b, a good accordance between the observed and simulated

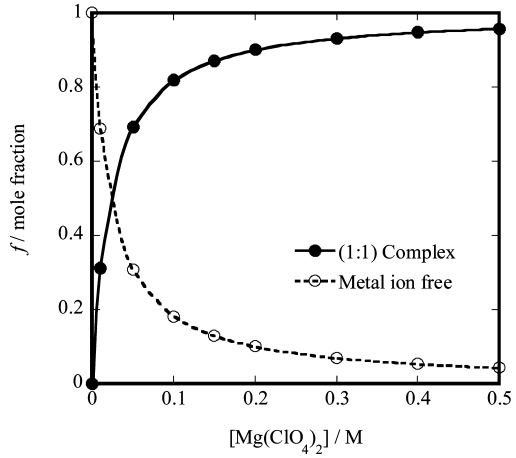

Figure 11. Plots of mole fractions of Mg^{2+}-free α-Toc• (f_{free}) (dotted line) and a (1:1) complex with α-Toc• ($f_{complex}$) (solid line) versus the concentration of $Mg(ClO_4)_2$ salt.

absorption spectra was observed. The result suggests that only the (1:1) complex coexists with Mg^{2+}-free α-Toc• in solution (see eq 10). The result of the DFT calculation also supports the present result (eq 8). Similar results were obtained for the Li^+ and Na^+ complexes by the DFT calculation. α-Toc• radical was stabilized by forming the (1:1) complex with metal cations (Mg^{2+}, Na^+, and Li^+) in acetonitrile solution.

4.3. Metal Cations Forming (1:1) Complexes with β-, γ-, and δ-Toc• Radicals and Hindering the Formation of Toc• Dimers in Acetonitrile Solution. As shown in Figure 7 and as listed in Table 2, the values of molar extinction coefficients (ε_{max}) of α-, β-, γ-, and δ-Toc• increased with increasing concentrations of metal salts and approached different constant values at high concentrations of metal salts. The ε_{max} value increased in the order of eq 7 at the same concentration of the metal salts for any Toc• radical.

The ε_{max} values of the α-, β-, γ-, and δ-Toc• radicals in acetonitrile solution including 0.00 and 0.50 M metal salts ($LiClO_4$, $NaClO_4$, and $Mg(ClO_4)_2$) at 25.0 °C and their ratios (ε_{max}(0.50 M)/ε_{max}(0.00 M)) are listed in Table 2. The effect of $Mg(ClO_4)_2$ salt on the ε_{max} value was the largest among three kinds of the salts. The values of the ratios (ε_{max}(0.50 M)/ε_{max}(0.00 M)) obtained for $Mg(ClO_4)_2$ were 1.35, 5.14, 10.4, and 12.1 for α-, β-, γ-, and δ-Toc• radicals, respectively. A notable increase of the ε_{max} values observed for β-, γ-, and δ-Toc• in the presence of metal salts will be explained in the following way.

As reported in previous works,[4,17,19,27,28] the decay of the α-Toc• follows the bimolecular self-reaction of α-Toc• radicals, suggesting the production of α-TocH and α-tocopherol-*o*-quinonemethide (α-Toc-QM) (see Figure 1)) by a disproportionation reaction (reaction 19).

$$\alpha\text{-Toc}^\bullet + \alpha\text{-Toc}^\bullet \xrightarrow{2k_d} \alpha\text{-TocH} + \alpha\text{-Toc-QM} \quad (19)$$

The ε_{max} values and decay rates ($2k_d$) of α-Toc• were exactly determined in several solvents.

On the other hand, most of the phenoxyl (PhO•) free radicals are unstable and decay by fast bimolecular reactions with each other. Bimolecular radical decay of PhO• radical involves dimerization (recombination) and disproportionation reactions.[34] Most of such dimers, for example, dimers of 2,6-di-*tert*-butyl-4-R- or 2,6-diphenyl-4-R-phenoxyl radicals (for

dx.doi.org/10.1021/jp305039z | J. Phys. Chem. B 2012, 116, 8930−8941

instance, R = CH_3 or C_2H_5), have structures of quinol ethers ("head-to-tail"). Dimerization reactions of PhO$^\bullet$ radicals are fast reactions and are characterized by large rate constants ($k \approx 10^7-10^9$ M^{-1} s^{-1}) in nonviscous solvents at room temperature.

α-Toc$^\bullet$ radical in *n*-hexane may also decay in two steps (dimerization and disproportionation), as observed for PhO$^\bullet$ radicals. First, an equilibrium for dimerization establishes itself very quickly (with k_{21} and k_{-21}), and then disproportionation reaction 19 with $2k_d$ follows (reaction 20), as proposed by Doba et al.[35] and ascertained by Lucarini and Pedulli.[17] The k_{21} and k_{-21} represent the rate constants for the formation and breakdown of the dimer, respectively.

$$(\alpha\text{-Toc}-\alpha\text{-Toc}) \underset{2k_{21}}{\overset{2k_{-21}}{\rightleftharpoons}} \alpha\text{-Toc}^\bullet + \alpha\text{-Toc}^\bullet \xrightarrow{2k_d} \alpha\text{-TocH} + \alpha\text{-Toc}-\text{QM} \quad (20)$$

where the α-Toc$^\bullet$ dimer (α-Toc−α-Toc) is quinol ether (see Figure 1), although it is unstable and has not been isolated.

As reported in previous works,[19,27,28] the decay curves of α-Toc$^\bullet$ in polar ethanol, acetonitrile, dichloromethane, and chloroform solvents were explained by a simple bimolecular reaction without the dimer formation. The strong interaction between the polar solvent and α-Toc$^\bullet$ molecules (and/or metal cations) will hinder the formation of the quinol−ether-type dimer of α-Toc$^\bullet$ radicals. On the other hand, in *n*-hexane, *n*-heptane, and diethylether solvents, α-Toc$^\bullet$ radicals are believed to form dimers quickly and then to disappear gradually by bimolecular reaction. The relative ratios of the dimer formation will increase with decreasing polarity of the solvents (dielectric constant), and thus, the values of ε_{max} decrease from ε_{max} = 4370 M^{-1} cm^{-1} in ethanol to 2500 M^{-1} cm^{-1} in *n*-hexane.[19]

In a previous work,[19] similar measurements were performed for β-, γ-, and δ-TocH in ethanol in order to determine the ε_{max} values and the $2k_d$ values for reaction 19. However, the absorbances of α-, β-, γ-, and δ-Toc$^\bullet$ observed decreased rapidly in the order of α-Toc$^\bullet$ > β-Toc$^\bullet$ > γ-Toc$^\bullet$ > δ-Toc$^\bullet$ in ethanol (see Figure 6 in ref 19). The smaller absorbance obtained for β-, γ-, and δ-Toc$^\bullet$ radicals will be due to the fast formation of dimer (fast equilibrium with the dimer) (reaction 20)) in these Toc$^\bullet$ radical molecules. The steric repulsion due to two *ortho*-methyl groups on the α-Toc$^\bullet$ radical molecule will hinder the formation of the quinol−ether-type dimer. However, the dimer formation will become easier with a decreasing number of *ortho*-methyl groups. As a result, the values of the absorbance decrease in the order of α-Toc$^\bullet$ > β-Toc$^\bullet$ > γ-Toc$^\bullet$ > δ-Toc$^\bullet$ radicals in ethanol solvent. In addition to the interaction between the solvent and Toc$^\bullet$ radical molecules, such steric hindrance will also have an important effect on the dimer formation. To our regret, we were unsuccessful in determining the ε_{max} values for β-, γ-, and δ-Toc$^\bullet$ radicals. However, we estimated tentatively the apparent ε_{max} values ($\varepsilon_{max}^{apparent}$ = 1500, 820, and 380 M^{-1} cm^{-1} for β-, γ-, and δ-Toc$^\bullet$ radicals, respectively) (see Table 3 in ref 19) by using the relation (Absorbance(at t_{max}) = ε_{max}[Toc$^\bullet$] = ε_{max}[ArO$^\bullet$]$_{t=0}$). Here, the apparent ε_{max} value was defined as ε_{max} for a mixture of the Toc$^\bullet$ monomer and quinol−ether-type Toc$^\bullet$ dimer.

In the present work, similarly, the apparent ε_{max} values (4320, 1170, 365, and ∼100 $M^{-1}cm^{-1}$) (see Table 2) were determined for α-, β-, γ-, and δ-Toc$^\bullet$ radicals, respectively, in acetonitrile. A remarkable increase of the apparent ε_{max} values of β-, γ-, and δ-Toc$^\bullet$ radicals in acetonitrile solution including metal salts (see Figure 7) will be due to the complex formation between Toc$^\bullet$ and metal cations. As the results of the analyses of the UV−vis absorption spectra and the DFT MO calculations indicate, α-, β-, γ-, and δ-Toc$^\bullet$ radicals are stabilized by the complex formation with metal cations. With increasing concentration of metal salts, the mole fraction of the metal complex will increase (see Figure 11), and thus, the formation of Toc$^\bullet$ dimer in the solution will be suppressed (see eqs 10 and 21). As a result, the ε_{max} values will increase. In fact, the rate constant ($2k_d$) of bimolecular reaction of α-Toc$^\bullet$ was also decreased by the complex formation, as reported in a previous work.[28]

$$2M^+ + (\alpha\text{-Toc}-\alpha\text{-Toc}) \underset{2k_{21}}{\overset{2k_{-21}}{\rightleftharpoons}} (\alpha\text{-Toc}^\bullet\cdots M^+) + (\alpha\text{-Toc}^\bullet\cdots M^+) \xrightarrow{2k_d} \alpha\text{-TocH} + \alpha\text{-Toc}-\text{QM} + 2M^+ \quad (21)$$

5. SUMMARY

As described in the Introduction, α-, β-, γ-, and δ-Toc$^\bullet$ radicals are important key radicals, which appear in the process of the antioxidant and pro-oxidant actions of α-, β-, γ-, and δ-TocH (see reactions 1−5). In recent years, detailed kinetic studies were performed for tocopherol regeneration reaction 3, bimolecular reaction 4, and free-radical-scavenging reaction 5, and the mechanisms involved and the effect of metal salts on the reaction rates (k_r, $2k_d$, and k_s) were studied. A notable effect of the solvent was observed for reactions 3−5 in the presence of metal salts.

In the present work, the measurements of the UV−vis absorption spectra of α-, β-, γ-, and δ-Toc$^\bullet$ radicals were performed in acetonitrile solution including three kinds of alkali and alkaline earth metal salts ($LiClO_4$, $NaClO_4$, and $Mg(ClO_4)_2$) (MX or MX_2). Remarkable effects of the metal salts were observed on the maximum wavelengths (λ_{max}) and molar extinction coefficient (ε_{max}) of the absorption spectra of the α-, β-, γ-, and δ-Toc$^\bullet$, suggesting (Toc$^\bullet\cdots M^+$ (or M^{2+})) complex formations. The stability constants (K) were determined for Li^+, Na^+, and Mg^{2+} complexes of α-, β-, γ-, and δ-Toc$^\bullet$. The alkali and alkaline earth metal salts having a smaller ionic radius and a larger charge of the cation gave a larger shift of the λ_{max} value, a larger ε_{max} value, and a larger K value. The result of the DFT calculations indicated that the α-, β-, γ-, and δ-Toc$^\bullet$ radicals were stabilized by the (1:1) complex formation between Toc$^\bullet$ and metal cations (Li^+, Na^+, and Mg^{2+}).

High concentrations of alkali and alkaline earth metal salts coexist with α-, β-, γ-, and δ-TocH in plasma, blood, and many tissues; for instance, the concentrations of metal cations included in mammals are [Na^+] = 140 mM, [K^+] = 4 mM, and [Mg^{2+}] = 1.5 mM in extracellular fluid and [Na^+] = 10 mM, [K^+] = 140 mM, and [Mg^{2+}] = 30 mM in intracellular fluids.[36] The concentrations in human blood are [Na^+] = 81.7 mM and [K^+] = 44.6 mM, and in human plasma, they are [Na^+] = 136 mM and [K^+] = 3.6 mM.[20] The concentration of α-TocH in human plasma was reported to be on average 22.0 (12.0−36.0) μM.[37] These facts suggest the contribution of the metal salts to the above key reactions in biological systems. Further kinetic study of the reactions 1−5 in micellar solution and liposome including metal salts will be necessary to clarify the effect of the metal salts in biological systems.

dx.doi.org/10.1021/jp305039z | J. Phys. Chem. B 2012, 116, 8930−8941

■ ASSOCIATED CONTENT

Supporting Information

The Mulliken atomic charges (Z) on oxygen and carbon atoms of the α-, β-, γ-, and δ-Toc$^{\bullet}$ model radicals obtained with the DFT calculations. This material is available free of charge via the Internet at http://pubs.acs.org.

■ AUTHOR INFORMATION

Corresponding Author

*Tel: 81-89-927-9588. Fax: 81-89-927-9590. E-mail: mukai-k@dpc.ehime-u.ac.jp.

Notes

The authors declare no competing financial interest.

■ ACKNOWLEDGMENTS

S.N. is grateful to Dr. Umpei Nagashima of the Japanese National Institute of Advanced Industrial Science and Technology and Professor Hiroyuki Teramae of Josai University for their valuable discussion on the computations. S.N. also thanks the Research Center for Computational Science at the Okazaki Research Facilities of the Japanese National Institute of Natural Science for the use of their computers and the Library Program Gaussian 09. This work was partly supported by a Grant-in-Aid for Challenging Exploratory Research (No. 24658123) from the Japan Society for the Promotion of Science.

■ REFERENCES

(1) Niki, E. *Chem. Phys. Lipids* **1987**, *44*, 227−253.
(2) Barclay, L. R. C. *Can. J. Chem.* **1993**, *71*, 1−16.
(3) Traber, M. G.; Atkinson, J. *Free Radical Biol. Med.* **2007**, *43*, 4−15.
(4) Burton, G. W.; Doba, T.; Gabe, E. J.; Hughes, L.; Lee, F. L.; Prasad, L.; Ingold, K. U. *J. Am. Chem. Soc.* **1985**, *107*, 7053−7065.
(5) Cillard, J.; Cillard, P.; Cormier, M.; Girre, L. *J. Am. Oil Chem. Soc.* **1980**, *57*, 252−255.
(6) Terao, J.; Matsushita, S. *Lipids* **1986**, *21*, 255−260.
(7) Nagaoka, S.; Okauchi, Y.; Urano, S.; Nagashima, U.; Mukai, K. *J. Am. Chem. Soc.* **1990**, *112*, 8921−8924.
(8) Bowry, V. W.; Stocker, R. *J. Am. Chem. Soc.* **1993**, *115*, 6029−6044.
(9) Mukai, K.; Noborio, S.; Nagaoka, S. *Int. J. Chem. Kinet.* **2005**, *37*, 605−610 and references cited therein.
(10) Ouchi, A.; Ishikura, M.; Konishi, K.; Nagaoka, S.; Mukai, K. *Lipids* **2009**, *44*, 935−943.
(11) *Coenzyme Q: Molecular mechanisms in health and disease*; Kagan, V. E., Quinn, P. J., Eds.; CRC Press: Boca Raton, FL, 2001.
(12) Mukai, K.; Itoh, S.; Morimoto, H. *J. Biol. Chem.* **1992**, *267*, 22277−22281.
(13) Ouchi, A.; Nagaoka, S.; Mukai, K. *J. Phys. Chem. B* **2010**, *114*, 6601−6607.
(14) Packer, J. E.; Slater, T. F.; Willson, R. L. *Nature* **1979**, *278*, 737−738.
(15) Bisby, R. H.; Parker, A. W. *Arch. Biochem. Biophys.* **1995**, *317*, 170−178.
(16) Nagaoka, S.; Kakiuchi, T.; Ohara, K.; Mukai, K. *Chem. Phys. Lipids* **2007**, *146*, 26−32.
(17) Lucarini, M.; Pedulli, G. F.; Cipollone, M. *J. Org. Chem.* **1994**, *59*, 5063−5070.
(18) Gregor, W.; Grabner, G.; Adelwhrer, C.; Rosenau, T.; Gille, L. *J. Org. Chem.* **2005**, *70*, 3472−3483.
(19) Mukai, K.; Ouchi, A.; Mitarai, A.; Ohara, K.; Matsuoka, C. *Bull. Chem. Soc. Jpn.* **2009**, *82*, 494−503 and references are cited therein.
(20) Takeda, R.; Nakamura, T.; Saito, Y.; Takeda, A.; Yamashita, C.; Shigetomi, H.; Takeda, T.; Kimura, M. *Biomed. Res. Trace Elem.* **2007**, *18*, 277−280.
(21) Stryer, L. *Biochemistry* 3rd ed.; W. H. Freeman and Company: New York, 1988.
(22) Jiang, Q.; Christen, S.; Shigenaga, M. K.; Ames, B. N. *Am. J. Clin. Nutr.* **2001**, *74*, 714−722 and references cited therein.
(23) Machlin, L. J. Vitamin, E. In *Handbook of Vatamins*; Machlin, L. J., Ed.; Marcel Dekker Inc.: New York, 1991; pp 99−144.
(24) Leonard, S. W.; Paterson, E.; Atkinson, J. K.; Ramakrishnan, R.; Cross, C. E.; Traber, M. G. *Free Radical Biol. Med.* **2005**, *38*, 857−866.
(25) Nakanishi, I.; Fukuhara, K.; Shimada, T.; Ohkubo, K.; Iizuka, Y.; Inami, K.; Mochizuki, M.; Urano, S.; Itoh, S.; Miyata, N.; Fukuzumi, S. *J. Chem. Soc., Perkin Trans. 2* **2002**, 1520−1524.
(26) Nakanishi, I.; Kawashima, T.; Ohkubo, K.; Kanazawa, H.; Inami, K.; Mochizuki, M.; Fukuhara, K.; Okuda, H.; Ozawa, T.; Itoh, S.; Fukuzumi, S.; Ikota, N. *Org. Biomol. Chem.* **2005**, *3*, 626−629.
(27) Ouchi, A.; Nagaoka, S.; Abe, K.; Mukai, K. *J. Phys. Chem. B* **2009**, *113*, 13322−13331 and references cited therein.
(28) Kohno, Y.; Fujii, M.; Matsuoka, C.; Hashimoto, H.; Ouchi, A.; Nagaoka, S.; Mukai, K. *J. Phys. Chem. B* **2011**, *115*, 9880−9888.
(29) Mukai, K.; Oi, M.; Ouchi, A.; Nagaoka, S. *J. Phys. Chem. B* **2012**, *116*, 2615−2621.
(30) Rieker, A.; Scheffler, K. *Liebigs Ann. Chem.* **1965**, *689*, 78−92.
(31) Frisch, M. J.; Trucks, G. W.; Schlegel, H. B.; Scuseria, G. E.; Robb, M. A.; Cheeseman, J. R.; Scalmani, G.; Barone, V.; Mennucci, B.; Petersson, G. A.; Nakatsuji, H.; Caricato, M.; Li, X.; Hratchian, H. P.; Izmaylov, A. F.; Bloino, J.; Zheng, G.; Sonnenberg, J. L.; Hada, M.; Ehara, M.; Toyota, K.; Fukuda, R.; Hasegawa, J.; Ishida, M.; Nakajima, T.; Honda, Y.; Kitao, O.; Nakai, H.; Vreven, T.; Montgomery, J. A., Jr.; Peralta, J. E.; Ogliaro, F.; Bearpark, M.; Heyd, J. J.; Brothers, E.; Kudin, K. N.; Staroverov, V. N.; Keith, T.; Kobayashi, R.; Normand, J.; Raghavachari, K.; Rendell, A.; Burant, J. C.; Iyengar, S. S.; Tomasi, J.; Cossi, M.; Rega, N.; Millam, J. M.; Klene, M.; Knox, J. E.; Cross, J. B.; Bakken, V.; Adamo, C.; Jaramillo, J.; Gomperts, R.; Stratmann, R. E.; Yazyev, O.; Austin, A. J.; Cammi, R.; Pomelli, C.; Ochterski, J. W.; Martin, R. L.; Morokuma, K.; Zakrzewski, V. G.; Voth, G. A.; Salvador, P.; Dannenberg, J. J.; Dapprich, S.; Daniels, A. D.; Farkas, O.; Foresman, J. B.; Ortiz, J. V.; Cioslowski, J.; , Fox, D. J. *Gaussian 09*, revision B.01; Gaussian, Inc.: Wallingford, CT, 2010.
(32) Fukuzumi, S.; Kuroda, S.; Tanaka, T. *J. Am. Chem. Soc.* **1985**, *107*, 3020−3027.
(33) Fukuzumi, S.; Ohkubo, K. *Chem.—Eur. J.* **2000**, *6*, 4532−4535.
(34) Denisov, E. T.; Khudyakov, I. V. *Chem. Rev.* **1987**, *87*, 1313−1357.
(35) Doba, T.; Burton, G. W.; Ingold, K. U.; Matsuo, M. *J. Chem. Soc., Chem. Commun.* **1984**, 461−462.
(36) Murray, R. K.; Granner, D. K.; Mayes, P. A.; Rodwell, V. W. Membranes: Structure, Assembly, and Function. *Harper's Biochemistry*, 25th ed.; McGraw-Hill: New York, 2000; Chapter 43, pp 505−533.
(37) Colome, C.; Artuch, R.; Vilaseca, M.-A.; Sierra, C.; Brandi, N.; Lambruschini, N.; Cambra, F. J.; Campistol, J. *Am. J. Clin. Nutr.* **2003**, *77*, 185−188.